

# Formation of Large Negative Deuterium Ion Beams at ELISE

D. Wunderlich<sup>a</sup>, R. Riedl, I. Mario, A. Mimo, U. Fantz, B. Heinemann and W. Kraus

Max-Planck-Institut für Plasmaphysik, Boltzmannstraße 2, 85748 Garching, Germany

## Abstract

Negative ion sources for neutral beam injection in fusion experiments are based on the surface production of  $H^-$  or  $D^-$  on caesiated low work function surfaces. In the last years it was demonstrated at the large RF driven ion source of the ELISE test facility that the requirements for the ITER NBI systems can be fulfilled in hydrogen. This is a big step towards the first operational period of ITER, planned for up to 2035. However, for the following operational period neutral beam systems working in deuterium are needed. Operation of negative hydrogen ion sources in deuterium is significantly more demanding than in hydrogen: the amount of co-extracted electrons is much higher and their increase during pulses is much more pronounced, limiting the achievable performance. This paper presents results of investigations aimed to improve the insight in the physics related to this isotope effect. Due to the higher atomic mass of deuterium, caesium is removed much more effectively from reservoirs at the walls, resulting in a depletion of these reservoirs and a strongly increased caesium density in the plasma. Additionally, a correlation between the fluxes of charged particles towards the inner ion source surfaces and the co-extracted electrons is identified.

## Introduction

The neutral beam injection (NBI) system at ITER will be used for heating and current drive [1, 2]. An essential part of the NBI beam line is the negative ion source, capable of delivering an extracted current of 57 A for 3600 s in deuterium operation and 66 A for 1000 s in hydrogen (corresponding to current densities of 286 A/m<sup>2</sup> and 329 A/m<sup>2</sup>, respectively) at a filling pressure of 0.3 Pa.

The development towards the negative ion sources for ITER NBI follows a R&D roadmap defined by the European domestic agency F4E [3, 4]. First step within this roadmap is the RF driven prototype source (0.3×0.6 m<sup>2</sup> with an extraction area of typically 6·10<sup>-3</sup> m<sup>2</sup>) [5]. The half-ITER-size ion source of the ELISE test facility (Extraction from a Large Ion Source Experiment, 1×1 m<sup>2</sup> with an extraction area of 0.1 m<sup>2</sup>) [6, 7] is an intermediate step towards the ITER NBI ion source (1×2 m<sup>2</sup> with an extraction area of 0.2 m<sup>2</sup>) [2, 8].

The main production process for negative hydrogen or deuterium ions in these ion sources is the surface process [9] in a low-temperature plasma ( $T_e \approx 1$  eV,  $n_e \approx 10^{17}$  m<sup>-3</sup>). Negative ions are produced mainly by conversion of hydrogen atoms impinging the caesiated low work function ( $\approx 2.2$  eV [10]) surface of the plasma grid (PG), the first grid of a multi-grid, multi-aperture extraction and acceleration system. Extraction of negative ions is accompanied by co-extraction of electrons; for ITER NBI a ratio of co-extracted electrons to extracted negative ions below one is envisaged.

---

<sup>a</sup> Author to whom correspondence should be addressed: dirk.wuenderlich@ipp.mpg.de

The caesium needed for decreasing the PG surface work function is evaporated into the ion source volume by one or more caesium ovens [8, 11]. The evaporation rate (up to several mg/h [5]) is adjusted by the temperature of the caesium reservoir within the oven. Caesium accumulates on the inner source surfaces and is redistributed during plasma pulses [12, 13]. Caesium present in the plasma volume is ionized to a large degree [14]. Compared to operation without caesium, in a well-caesiated source the extracted ion current is up to a factor of ten higher and the co-extracted electron current is significantly reduced [15].

Operation in deuterium is much more demanding than in hydrogen [16]: The extracted negative ion current is similar but the amount of co-extracted electrons is significantly larger [5]. While during pulses the extracted ions are almost stable in both isotopes, the temporal increase in the co-extracted electron current is much more pronounced in deuterium than in hydrogen. The amount of co-extracted electrons and their temporal increase during pulses can strongly restrict operational parameters like the extraction potential or the RF power and consequently the number of extracted negative ions.

In a well-caesiated source the electronegativity of the plasma close to the extraction system is high and electrons are a minority species. Small changes in the PG surface work function caused by reactions with impurities embedded into or deposited on the caesium layers (from the background gas or the plasma) or by removal of caesium can result in a drastic increase in the co-extracted electrons. The deterioration of the work function can be counteracted by the interaction of the caesiated PG surface with the plasma [17] or by a sufficient caesium flux onto the surface [10]. Up to now, identical experimental measures have been applied for reducing and stabilizing the co-extracted electrons in hydrogen and deuterium, namely increasing the strength of the magnetic filter [18] and the caesium evaporation rate [19]. At ELISE additionally the positive effect of so-called potential rods is exploited [19]. While for hydrogen it is possible to demonstrate ITER relevant long pulses (1000 s plasma, pulsed extraction) [20], in deuterium up to now  $\approx 66\%$  of the ITER target for the extracted negative ion current density have been achieved over one hour.

This triggered dedicated investigations on the physics of the isotope effect. Main aim is to identify measures resulting in a caesium flux onto the PG sufficient to ensure in deuterium operation a low and homogeneous PG work function that is stable over pulses up to one hour, correlating with a low and stable co-extracted electron current and a high extracted negative ion current.

### The ELISE test facility

A schematic view of the ELISE ion source is shown in Figure 1. The plasma is generated by inductive RF coupling into four cylindrical drivers ( $P_{RF} < 75$  kW/driver, delivered by two RF

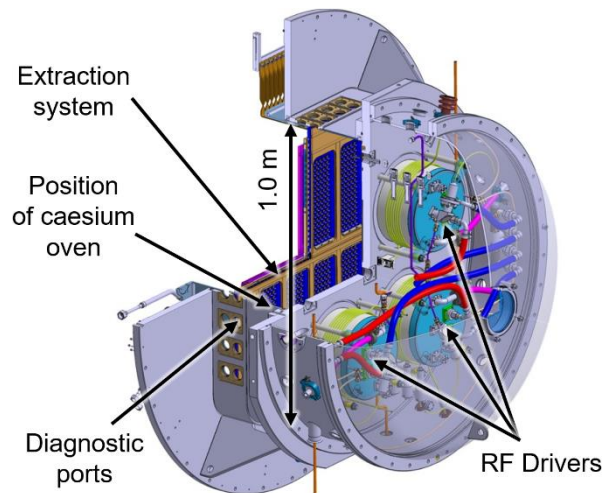


*Figure 1: Schematic view of the ELISE ion source. The position of one of the caesium ovens at the left vertical sidewall is indicated, the second oven is located at the right source wall.*

generators,  $f=1$  MHz) and then expands toward the extraction system. ELISE is operated in pulsed extraction mode: CW plasma pulses are possible, with short extraction blips (length: 9.5 s; the shortest possible time between two blips is  $\approx 150$  s, limited by the available HV power supply).

The co-extracted electrons are magnetically deflected onto the surface of the second grid, the extraction grid (EG). If the power deposited onto the EG is too high, beam extraction is stopped by a safety interlock. The design limit of power deposited onto the extraction grid is 200 kW per segment [6]. The safety interlock takes effect at 125 kW/segment in order to take into account possible non-homogeneities of the deposited power.

The horizontal magnetic filter field with a strength of a few mT (sufficient for magnetizing electrons but not the ions) plays a crucial role for the suppression of the co-extracted electrons (by a factor of up to ten, depending on the source parameters) and for the transport of negative hydrogen ions to the extraction apertures [21]. The magnetic filter is generated by a current,  $I_{PG}$ , flowing through the PG in vertical direction [22]. By varying  $I_{PG}$ , the strength of the filter field can be adjusted (up to 5.3 kA at maximum, equivalent to a field strength of  $\approx 5$  mT close to the PG). The filter field is strengthened and its topology modified by external permanent magnets attached to the vertical sidewalls of the source [18], adding in the center of the PG  $\approx 0.4$  mT to the filter strength. An additional reduction of the co-extracted electrons is obtained by a positive bias potential applied to the PG with respect to the source body and the so-called bias plate [5].

Two caesium ovens are attached to the sidewalls of ELISE; the Cs evaporation is monitored by surface ionization detectors (SID) at the oven nozzles [11]. The neutral caesium density close to the PG (2 cm axial distance) is diagnosed using Tunable Diode Laser Absorption Spectroscopy (TDLAS) [23].

### Isotope effect between hydrogen and deuterium.

The isotope effect between hydrogen and deuterium is illustrated in Figure 2. Shown in Figure 2a and b is the dependence of the electrically measured extracted negative ion current density  $j_{ex}$  and co-extracted electron current density  $j_e$  on the RF power  $P_{RF}$  for short pulses ( $t_{plasma}=20$  s, one extraction blip of 9.5 s) in hydrogen and deuterium. Each point represents an averaged measurement result (over the second half of an extraction blip in order to omit potential instabilities at the beginning of the blip). The shaded gray area indicates high performance operation, i.e. the elevated levels of  $P_{RF}$  needed for obtaining high extracted current densities.

Comparable parameters have been used for both isotopes (bias current=35 A, extraction voltage  $U_{ex}=7$  kV). The magnetic filter strength has been increased from  $\approx 1.9$  mT (hydrogen) to  $\approx 4.2$  mT (deuterium) in order to stabilize the co-extracted electrons, resulting in a reduction of also  $j_{ex}$ .

In hydrogen,  $j_{ex}$  and  $j_e$  increase in a comparable way with  $P_{RF}$  (Figure 2a), i.e. when increasing  $P_{RF}$  (and the extracted negative ion current) the electron-ion ratio is almost constant. In deuterium  $j_{ex}$  increases with  $P_{RF}$  but this increase flattens for  $P_{RF} \geq 50$  kW/driver (Figure 2b). In parallel,  $j_e$  increases dramatically in the high-performance region. Results of non-RF-compensated Langmuir pin probes indicate that the increase in  $j_e$  is correlated with an increase in the electron density close to the PG. The flattening of  $j_{ex}$  vs.  $P_{RF}$  is most probably a second order effect (due plasma quasi-neutrality).

Shown in Figure 2c and d are time traces of  $j_{ex}$  and  $j_e$  for the best short pulses (highest  $j_{ex}$ ) done up to now in hydrogen and deuterium. The maximum available RF power (75 kW/driver) is used. In hydrogen, the filter field strength is  $\approx 1.7$  mT in the center of the PG, in deuterium  $\approx 4.0$  mT. In hydrogen (Figure 2c)  $j_{ex}$  is almost constant over time.  $j_e$  increases only slightly and the power deposited onto the EG at the pulse end is well below 100 kW for each of the two grid segments, i.e.  $j_{ex}$  is limited only by the available RF power and by the limit of the used HV power supply,  $I_{max} \approx 30$  A.

In deuterium (Figure 2d)  $j_{ex}$  is significantly lower than in

hydrogen which is an effect of the increased filter strength. Additionally, it decreases visibly during the extraction blip. The co-extracted electrons strongly increase over the pulse length and the power on the EG approaches the set limit. The caesium evaporation rate ( $\approx 4$  mg/h is an upper limit estimated from the SID signals) is significantly higher than in hydrogen or in deuterium operation at lower RF power ( $\approx 1.7$  mg/h were reported for initial caesium conditioning in deuterium at  $P_{RF} = 21$  kW/driver [24]). The two interrupts in the signals at  $\approx 14$  s are caused by HV breakdowns in the extraction system, most probably triggered by the presence of Cs. These indicate that increasing much further the amount of caesium in the plasma is not possible since this could increase the amount of breakdowns to a non-acceptable level.

### Physics differences between operation in hydrogen and in deuterium

For the very first time, the operational gas was changed from hydrogen to deuterium within one operational day. Using identical source parameters,  $P_{RF}$  was set to 50 kW/driver, the filter field to  $\approx 2.7$  mT and the extraction voltage to 7 kV, i.e. parameters for which in deuterium operation the co-extracted electrons can be handled.

Figure 3a shows  $j_{ex}$  and  $j_e$ , plotted in Figure 3b is the neutral Cs density from TDLAS. Again, each point represents an averaged measurement result. The vertical dashed line illustrates the time of switching the isotope.

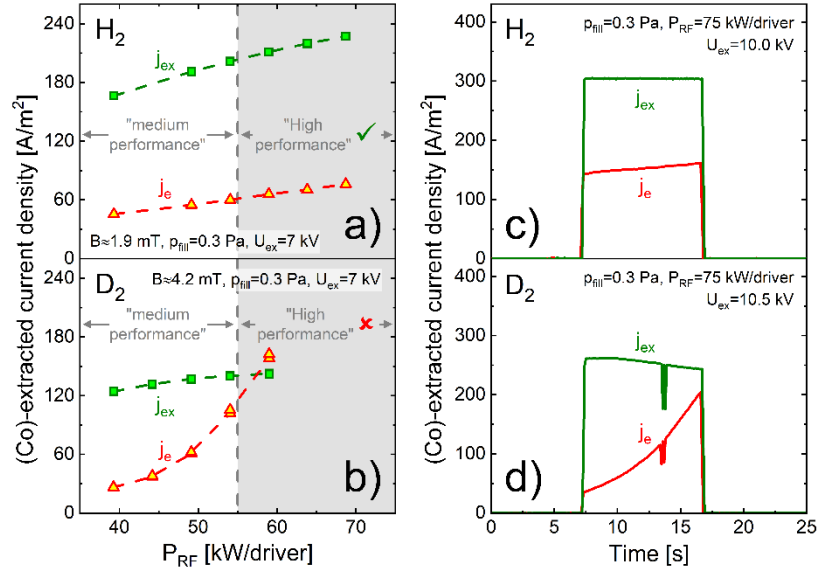


Figure 2: Isotope effect between hydrogen and deuterium: a) and b): dependence of extracted ions and co-extracted electrons on the RF power. c) and d): time traces of the extracted negative ion current and the co-extracted electron current for the short pulses (one extraction blip) with the highest  $j_{ex}$  (for  $j_e/j_{ex} < 1$ ) achieved up to now at ELISE.

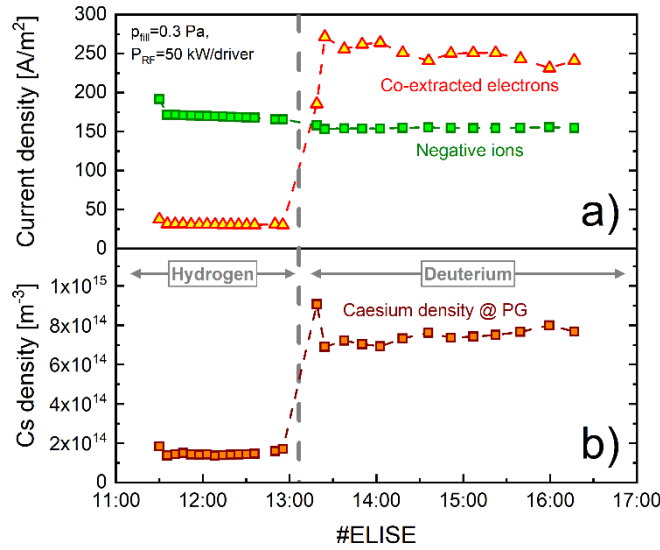


Figure 3: Signals taken during one operational day when switching from  $H_2$  to  $D_2$  for identical source parameters. a) Extracted negative ion current and co-extracted electron current. b) Cs density close to the plasma grid surface from TDLAS.

The ratio of ionic to neutral caesium is comparable for the two isotopes (justified by comparable electron temperatures and densities [25]), this indicates a strongly enhanced caesium removal from reservoirs at the ion source walls, most probably caused by the higher mass of deuterium.

The first pulse in  $D_2$  shows an overshoot in  $n(Cs)$ , indicating that the enhanced caesium removal depletes the reservoirs at the walls. This is illustrated additionally by Figure 4, showing traces of  $n(Cs)$  for the last pulse in hydrogen and some of the subsequent deuterium pulses. The ripple on the time traces is most probably caused by a ripple of the laser wavelength. In hydrogen,  $n(Cs)$  is comparatively low ( $2 \cdot 10^{14} \text{ m}^{-3}$ ) and stable. In deuterium,  $n(Cs)$  is by a factor of up to 7 higher, significantly more unstable and the impact of the back streaming positive ions (releasing during extraction blips caesium deposited at the source back plate [26]) is more pronounced.  $n(Cs)$  at the pulse beginning decreases significantly between the first and second pulse in deuterium. It is stabilized and slightly enhanced only by the increased caesium fluence. The saturation level of  $n(Cs)$  at the pulse end (by a factor  $\approx 3$  higher than in hydrogen) is almost not

$j_{ex}$  almost does not depend on the isotope, indicating a comparable general caesium conditioning status. In contrast,  $j_e$  increases by a factor of  $\approx 6$  (first pulse in  $D_2$ ) up to  $\approx 9$  (second and subsequent pulses). It can be stabilized only by prolonging the break between two pulses from 5 minutes to 17 minutes, increasing the Cs fluence (the caesium amount evaporated between the pulses). However, within the extraction blips still a strong temporal dependence is observed:  $j_{ex}$  decreases by  $\approx 10\%$  during the 9.5 s of an extraction blip,  $j_e$  increases by a factor of  $\approx 3$  (not shown).

The caesium evaporation measured by the SID (not shown) increases only slightly when switching to deuterium while the neutral caesium density close to the PG increases by almost a factor of four. Assuming that the

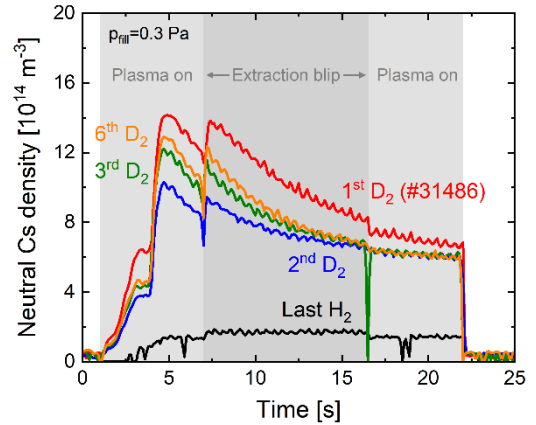


Figure 4: Time traces of  $n(Cs)$  close to the plasma grid surface measured using TDLAS for the last pulse before switching from  $H_2$  to  $D_2$  and for four different pulses in  $D_2$  with increasing Cs fluence evaporated between these pulses. The grey shaded areas symbolize the duration of the plasma phase and the extraction blip.

affected by the increased fluence and obviously it is not sufficient for stabilizing the co-extracted electrons.

It has to be kept in mind that not  $n(\text{Cs})$  but the surface work function of the PG is the relevant parameter for the source performance. The work function is the result of adsorption of Cs (and impurities), surface cleaning and caesium desorption. The present results indicate that the higher atomic mass of deuterium drastically shifts the equilibrium between Cs adsorption and desorption.

### Stabilizing and reducing the co-extracted electrons in deuterium

Figure 5 compares characteristics of an RF-compensated Langmuir probe located close to the PG for three pulses done using identical RF power (40 kW/driver): in hydrogen and deuterium for an identical filter field strength ( $\approx 3.2$  mT in the center of the PG, close to the highest field strengths typically used in hydrogen but too low for deuterium) and in deuterium with a strengthened filter field ( $\approx 4.6$  mT), resulting in reduced and stabilized  $j_e$ .

Switching from hydrogen (green curve) to deuterium (blue curve and red curve) increases the plasma potential by  $\approx 10$  V, independent of the filter strength, affecting the potential difference between plasma and the sidewalls. Additionally, the difference between plasma potential and the local PG (bias) potential changes:  $(\phi_{\text{PG}} - \phi_{\text{plasma}})$  is  $\approx 3$  V in hydrogen, it decreases to  $\approx 1$  V in deuterium when the filter strength is not adjusted and increases to  $\approx 3$  V when strengthening the filter. These results demonstrate that i) the fluxes of charged particles towards the surfaces and consequently the composition of the plasma depend on the used isotope ii) a higher potential difference between the PG and the plasma correlates with a better suppression of co-extracted electrons in deuterium. It has to be kept in mind, however, that the local probe measurement determines the potential difference only at one specific location of the large area PG.

The correlation between the potential differences and the plasma composition is supported by the different probe characteristics: in hydrogen the characteristics is almost symmetric w.r.t. the plasma potential, indicating a high electronegativity, i.e. an ion-ion plasma. After switching to deuterium, the characteristics is strongly asymmetric: the electron branch is much higher than the positive ion branch, indicating a high electron density close to the PG. When strengthening the magnetic filter, the electronegativity of the plasma increases but an ion-ion plasma is not achieved: the currents measured in the electron branch are higher than in the ion branch.

The charged particle fluxes towards the source surfaces can be affected not only by the strength but also by the topology of the magnetic filter field. The next step in investigating possible measures for stabilizing and reducing in deuterium

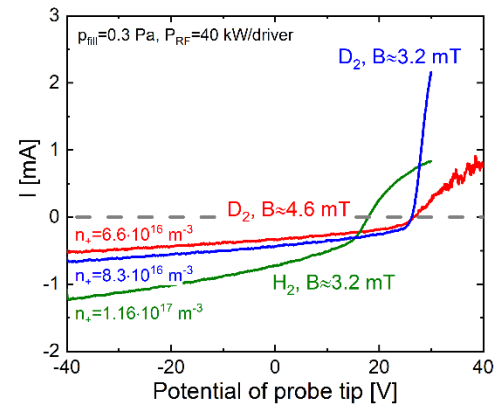


Figure 5: Probe characteristics measured in hydrogen and deuterium for identical source parameters. For the second deuterium pulse, the magnetic filter strength was increased in order to compensate for the instability of the co-extracted electrons.



the co-extracted electrons included modifications of the filter field structure. Up to now, no significant improvement of the behavior of the co-extracted electrons in deuterium was achieved.

## Summary and conclusions

Up to now, at ELISE 66 % of the ITER target for the extracted current density could be demonstrated during long (up to one hour) deuterium pulses at ELISE. The fact that this factor is significantly lower than what can be achieved in hydrogen is caused by a strong isotope effect between  $H_2$  and  $D_2$ . While the extracted ion current is almost not affected, in deuterium the co-extracted electrons are dramatically enhanced and destabilized, especially for high source performance, i.e. high RF power (and extraction potential).

Dedicated investigations show that in deuterium the caesium removal from reservoirs on the ion source walls is strongly enhanced and that the amount of Cs in the plasma needed for stabilizing the co-extracted electrons in deuterium is significantly higher than in hydrogen.

Langmuir probe measurements demonstrate that stabilizing the co-extracted electrons (by increasing the strength of the magnetic filter) is correlated to small changes in the sheath drop at the PG, affecting the flux of charged particles onto the PG surface. The main challenge for the future will be to identify measures for actively controlling such small physics changes resulting in a reduction and stabilization of the co-extracted electrons. These investigations will be supported by a computational model for the caesium transport and by a 3D Particle-In-Cell code describing self-consistently the plasma properties of a small region close to one extraction aperture.

## References

- [1] HEMSWORTH, R.; DECAMPS, H.; GRACEFFA, J.; SCHUNKE, B.; TANAKA, M.; DREMEL, M.; TANGA, A.; DE ESCH, H.P.L.; GELI, F.; MILNES, J. et al.; Status of the ITER heating neutral beam system, **Nucl. Fusion** **49**, 2009, 045006.
- [2] SINGH, M.J.; BOILSON, D.; HEMSWORTH, R.; CHAREYRE, J.; DECAMPS, H.; GELI, F.; GRACEFFA, J.; SCHUNKE, B.; SVENSSON, L.; SHAH, D. et al.; Heating Neutral Beams for ITER: Present Status, **IEEE Trans. Plasma Sci.** **44**, 2016, 1496.
- [3] MASIELLO, A.; AGARICI, G.; BONICELLI, T.; SIMON, M.; ANTONI, V.; DE ESCH, H.P.L.; LORENZI, A.; DREMEL, M.; FRANZEN, P.; HEMSWORTH, R. et al.; European programme towards the 1 MeV ITER NB injector, **Fusion Eng. Des.** **84**, 2009, 1276.
- [4] MASIELLO, A.; AGARICI, G.; BONICELLI, T.; FANTINI, F.; GAGLIARDI, M.; PAOLUCCI, M.; SIMON, M.; WIKUS, P.; AGOSTINETTI, P.; BIGI, M. et al.; Proc. 24th IAEA Fusion Energy Conference, San Diego, USA, 2012.
- [5] HEINEMANN, B.; FANTZ, U.; KRAUS, W.; SCHIESKO, L.; WIMMER, C.; WÜNDERLICH, D.; BONOMO, F.;

- FRÖSCHLE, M.; NOCENTINI, R.; RIEDL, R.; Towards large and powerful radio frequency driven negative ion sources for fusion, **New Journal of Physics** **19**, 2017, 015001.
- [6] HEINEMANN, B.; FALTER, H.D.; FANTZ, U.; FRANZEN, P.; FRÖSCHLE, M.; GUTSER, R.; KRAUS, W.; NOCENTINI, R.; RIEDL, R.; SPETH, E. et al.; Design of the "half-size" ITER neutral beam source for the test facility ELISE, **Fusion Eng. Des.** **84**, 2009, 915.
- [7] FRANZEN, P.; HEINEMANN, B.; FANTZ, U.; WÜNDERLICH, D.; KRAUS, W.; FRÖSCHLE, M.; MARTENS, C.; RIEDL, R.; NOCENTINI, R.; MASIELLO, A. et al.; Commissioning and first results of the ITER-relevant negative ionbeam test facility ELISE, **Fusion Eng. Des.** **88**, 2013, 3132.
- [8] TOIGO, V.; PIOVAN, R.; BELLO, S.; DALGAIO, E.; LUCHETTA, A.; PASQUALOTTO, R.; ZACCARIA, P.; BIGLI, M.; CHITARIN, G.; MARCUZZI, D. et al.; The PRIMA Test Facility: SPIDER and MITICA test-beds for ITER neutral beam injectors, **New J. Phys.** **19**, 2017, 085004.
- [9] BACAL, M.; Physics aspects of negative ion sources, **Nucl. Fusion** **46**, 2006, S250.
- [10] GUTSER, R.; WIMMER, C.; FANTZ, U.; Work function measurements during plasma exposition at conditions relevant in negative ion sources for the ITER neutral beam injection, **Rev. Sci. Instrum.** **82**, 2011, 023506.
- [11] FRÖSCHLE, M.; RIEDL, R.; FALTER, H.D.; GUTSER, R.; FANTZ, U.; THE NNBI-TEAM; Recent developments at IPP on evaporation and control of caesium in negative ion sources, **Fusion Eng. Des.** **84**, 2009, 788.
- [12] GUTSER, R.; WÜNDERLICH, D.; FANTZ, U.; THE NNBI-TEAM; Dynamics of the transport of ionic and atomic cesium in radio frequency-driven ion sources for ITER neutral beam injection, **Plasma Phys. Control. Fusion** **53**, 2011, 105014.
- [13] MIMO, A.; WIMMER, C.; WÜNDERLICH, D.; FANTZ, U.; Modelling of caesium dynamics in the negative ion sources at BATMAN and ELISE, **AIP Conf. Proc.** **1869**, 2017, 030019.
- [14] FANTZ, U.; FALTER, H.D.; FRANZEN, P.; BANDYOPADHYAY, M.; HEINEMANN, B.; KRAUS, W.; MCNEELY, P.; RIEDL, R.; SPETH, E.; TANGA, A. et al.; Diagnostics of the cesium amount in an RF negative ion source and the correlation with the extracted current density, **Fusion Eng. Des.** **74**, 2005, 299.
- [15] SPETH, E.; FALTER, H.D.; FRANZEN, P.; FANTZ, U.; BANDYOPADHYAY, M.; CHRIST, S.; ENCHEVA, A.; FRÖSCHLE, M.; HOLTUM, D.; HEINEMANN, B. et al.; Overview of the RF source development programme at IPP Garching, **Nucl. Fusion** **46**, 2006, S220.
- [16] FRANZEN, P.; FANTZ, U.; WÜNDERLICH, D.; HEINEMANN, B.; RIEDL, R.; KRAUS, W.; FRÖSCHLE, M.; RUF, B.; NOCENTINI, R.; THE NNBI-TEAM; Progress of the ELISE test facility: Results of caesium



operation with low RF power, **Nucl. Fusion** **55**, 2015, 053005.

- [17] FRIEDL, R.; FANTZ, U.; Influence of H<sub>2</sub> and D<sub>2</sub> plasmas on the work function of caesiated materials, **J. Appl. Phys.** **122**, 2017, 083304.
- [18] WÜNDERLICH, D.; KRAUS, W.; FRÖSCHLE, M.; RIEDL, R.; FANTZ, U.; HEINEMANN, B.; THE NNBI-TEAM; Influence of the magnetic field topology on the performance of the large area negative hydrogen ion source test facility ELISE, **Plasma Phys. Control. Fusion** **58**, 2016, 125005.
- [19] WÜNDERLICH, D.; RIEDL, R.; BONOMO, F.; MARIO, I.; FANTZ, U.; HEINEMANN, B.; KRAUS, W.; NNBI-TEAM; Long pulse operation at ELISE: Approaching the ITER parameters, **AIP Conf. Proc.** **2052**, 2018, 040001.
- [20] WÜNDERLICH, D.; RIEDL, R.; BONOMO, F.; MARIO, I.; FANTZ, U.; HEINEMANN, B.; KRAUS, W.; Achievement of ITER-relevant accelerated negative hydrogen ion current densities over 1000 s at the ELISE test facility, **Nucl. Fusion** **59**, 2019, 084001.
- [21] FRANZEN, P.; SCHIESKO, L.; FRÖSCHLE, M.; WÜNDERLICH, D.; FANTZ, U.; THE NNBI-TEAM; Magnetic Filter Field Dependence of the Performance of the RF Driven IPP Prototype Source for Negative Hydrogen Ions, **Plasma Phys. Control. Fusion** **53**, 2011, 115006.
- [22] FRÖSCHLE, M.; FANTZ, U.; FRANZEN, P.; KRAUS, W.; NOCENTINI, R.; SCHIESKO, L.; WÜNDERLICH, D.; NNBI-TEAM; Magnetic filter field for ELISE – Concepts and design, **Fusion Eng. Des.** **88**, 2013, 1015.
- [23] WIMMER, C.; LINDAUER, M.; FANTZ, U.; Determination of the Cs distribution along a line of sight by the Zeeman splitting in an inhomogeneous magnetic field, **J. Phys. D** **51**, 2018, 395203.
- [24] WÜNDERLICH, D.; RIEDL, R.; FANTZ, U.; HEINEMANN, B.; KRAUS, W.; NNBI-TEAM; Initial caesium conditioning in deuterium of the ELISE negative ion source, **Plasma Phys. Control. Fusion** **60**, 2018, 085007.
- [25] FANTZ, U.; SCHIESKO, L.; WÜNDERLICH, D.; NNBI-TEAM; A Comparison Of Hydrogen And Deuterium Plasmas In The IPP Prototype Ion Source For Fusion, **AIP Conf. Proc.** **1515**, 2013, 187.
- [26] SCHIESKO, L.; HOPF, C.; FRANZEN, P.; KRAUS, W.; RIEDL, R.; FANTZ, U.; NNBI-TEAM; A study on backstreaming positive ions on a high power negative ion source for fusion, **Nucl. Fusion** **51**, 2011, 113021.